

Towards a new cosmological Milky Way like galaxy simulation in the Gaia Era

S. Roca-Fàbrega¹, O. Valenzuela², and F. Figueras¹

¹ Departament d'Astronomia i Meteorologia and IEEC-UB, Institut de Ciències del Cosmos de la Universitat de Barcelona, Martí i Franquès, 1, E-08028 Barcelona.

² Instituto de Astronomía, Universidad Nacional Autónoma de México, A.P. 70-264, 04510, México, D.F.; Ciudad Universitaria, D.F., México.

Abstract

We present a new cosmological Milky Way (MW) like galaxy formation simulation including N-body + hydrodynamics using the adaptive mesh refinement (AMR) code ART [14, 15]. The system has been evolved inside a 28 Mpc cosmological box with a spatial resolution of 109 pc. At $z = 0$ the system has an $M_{\text{vir}} = 7.33 \times 10^{11} M_{\odot}$. A well defined disk is formed inside the dark matter halo and the overall amount of gas and stars is comparable with MW observations. Several non-axisymmetric structures arise out of the disk (spirals, bars and warp) and also a thick disk component. Furthermore, a huge reservoir of hot gas is present at large distances from the disk, embedded in the dark matter halo. Our preliminar results reveal that the hot gas has a clearly anisotropic distribution and can be a part of the missing baryons in galaxies [10, 11].

1 Introduction

To simulate a system that fits the properties observed for our own Galaxy is not trivial. One of the most challenging problems in Λ CDM cosmological simulations in recent years has been to obtain realistic Milky Way (MW) like systems. It has been specially difficult to get models with extended disks and with a proper stellar age distributions, star formation rates and baryonic fractions that fit within the observations. Nowadays the N-body plus hydrodynamics codes are evolving to a better understanding of physical processes and thus to fit better MW observations. Important issues have been addressed in the last decade like disk formation or central bulge concentrations. In the recent years several authors [19, 8, 1, 4, 6, 9] obtained realistic rotationally supported disks with the properties of late-type spirals like MW. However most of these works have systems with too peaked rotation curves in the center. Some of them

[1] showed that to avoid the formation of these peaked systems exist some key parameters, the star formation efficiency and the gas density star formation threshold. They argue that to use a proper value for these parameters is necessary to reproduce the subgrid physics of star formation in molecular clouds. A combination of both parameters allow the system to consume the gas in the star formation region fast enough to ensure that the energy provided by SNe is not radiated too fast by the gas cooling. Simulations in the most recent works have reached very high levels of realism when comparing them with observations for the MW (e.g. [9, 2, 17]).

Here we present a set of new realistic MW like models with extended disks and unpeaked slowly decreasing rotation curves. We reach similar or better levels of realism as the most recent presented works but using an Eulerian, AMR approach. These models can be discussed in the context of the most competitive recent collaborative efforts.

2 General properties of our MW like models

We present three of our models that only differ in their refinement criteria and that are the ones that best fit the properties of our MW galaxy. Model HART321 is the one with a lightest refinement, HART322 has intermediate conditions and HART323 is the one with hardest refinement conditions (harder means that code splits cells easier). Parameters we present here are summarised and compared with recent MW like models and with observational values in Table 6.1 of Roca-Fàbrega PhD thesis.

At $z \sim 0$ our three models are late type massive spiral galaxies with several non-axisymmetric disk structures such as bars or spirals. Their assembling history is quiet after $z=1.5$ and the last major merger occurs at $z = 3$.

We observe that in all our models young stellar component (0–4 Gyr) is distributed in a flat disk structure. Older stellar populations (4–10 Gyr) are also distributed into a disk structure but in these cases this structure is not as flat as in the young case. We argue that disk scale height and length is that stellar population has an evident flare that is more evident for older populations. The younger stellar population also shows the presence of rings, spiral arms and also a young bar, in the disk. The gas components are placed in different regions of the system depending on its temperature: cold gas is present in the young stellar disk region and hot gas fills the out-of-plane region and is embedded in the DM halo. It is also interesting that cold/intermediate gas has a warped structure that is not observable in the stellar component.

Here we define the virial radius (r_{vir}) as the one where the sphere of radius r_{vir} encloses a mean density 97 times denser than the critical density (ρ_{crit}) of a spatially flat Universe $\rho_{\text{crit}} = 3H^2(z)/(8\pi G)$. We have obtained that the virial radius at $z = 0$ is $r_{\text{vir}} \sim 230$ kpc in all our three models and that the mass enclosed in this radius is $M_{\text{vir}} = 7.20\text{--}7.33 \times 10^{11} M_{\odot}$. This value for the M_{vir} what falls well inside the observational range that is $M_{\text{vir}}=0.6\text{--}2.4 \times 10^{12} M_{\odot}$ by [22, 3, 12]. This total mass is distributed in dark, stellar and gaseous matter as follows: $M_{\text{DM}} = 5.86\text{--}6.48 \times 10^{11} M_{\odot}$, $M_{\star} = 6.1\text{--}6.2 \times 10^{10} M_{\odot}$ and $M_{\text{gas}} = 1.73\text{--}2.70 \times 10^{10} M_{\odot}$. The baryonic fraction of our models is $f_{\text{b}} = 0.104\text{--}0.121$, these values are 19–31% smaller than the universal value for the adopted cosmology which is 0.15. The baryonic fraction obtained

when including all gas components is higher than the one observed for the MW, partially solving the missing baryons problem. The number of stellar particles and gas cells inside r_{vir} are $N_* = 0.4\text{--}2.3 \times 10^6$ and $N_{\text{gas}} = 0.2\text{--}1.4 \times 10^7$. All dark matter particles inside virial radius belong to less massive DM species and have a mass of $9.25 \times 10^4 M_\odot$. Star particles have masses between $\sim 10^3$ and $1.2 \times 10^6 M_\odot$.

The total rotation curve and its components of several models computed using the $\sqrt{GM_{<r}/r}$ approach are shown in Fig. 1. As can be seen in the figure our models show a very good fit within the most recent observational data. The peak of $z = 0$ circular velocity of our models is reached at $R_{\text{peak}} \sim 5.69$ kpc with a value of $V_c(R_{\text{peak}}) = 237.5\text{--}243.8 \text{ km s}^{-1}$; the value at a standard solar radius ($R_\odot = 8$ kpc) is $V_{c_\odot} = 233.6\text{--}239.8 \text{ km s}^{-1}$. Also the ratio between circular velocity at 2.2 times disk scale radius ($V_{2.2}$) and circular velocity at r_{200} (V_{200}) is well inside the observational range for the MW, that is $1.67^{+0.31}_{-0.24} \text{ km s}^{-1} \text{--} 1.11^{+0.22}_{-0.20} \text{ km s}^{-1}$ [22, 5], while we obtain $V_{2.2}/V_{200} \sim 1.9 \text{ km s}^{-1}$. Despite of the rotation and circular velocity curves we present here fit well inside observational ranges it is important to take into account that observational uncertainties are high.

3 Unraveling properties of MW like models

3.1 Hot gas component

3.1.1 Spatial distribution

The amount of hot gas ($T > 3 \times 10^5 \text{ K}$) in our models is in between $M_{\text{hot}} = 0.98\text{--}1.5 \times 10^{10} M_\odot$. This hot gas is X-ray luminous and it is embedded in the dark matter halo but mostly outside the stellar disk. In Fig. 2 we show a full sky view of the hot gas distribution in our model HART321. This figure has been obtained computing the column density of the hot gas from a position that is at 8 kpc from the galactic center, inside the simulated galactic disk and at an arbitrary azimuthal angle. Values fall well inside the observational ranges [10]. From Fig. 2 we note that the distribution of hot gas is far from isotropic. Another interesting result is that the gas distribution is not symmetric with respect to the disk plane what suggest some degree of interaction with the extragalactic medium.

3.1.2 Total hot gas mass: simulations vs. observations

It is difficult to infer the total hot gas mass in the MW when we have information only about its distribution in a few directions what is usual when using observations. In simulations it is easy to obtain the real hot gas distribution and from it, using the same approaches as in observational works, its real mass. To compute the total baryonic mass in real galaxies it is usually used to assume an spherically uniform gas distribution where the density is taken as being the mean value from all observations. This assumption gives the exact solution when the real gas density distribution is known i.e. an infinite number of observations that cover the full sky are available. In this context we have designed a test to determine the number of observations randomly distributed in the sky that are needed to recover the total hot gas

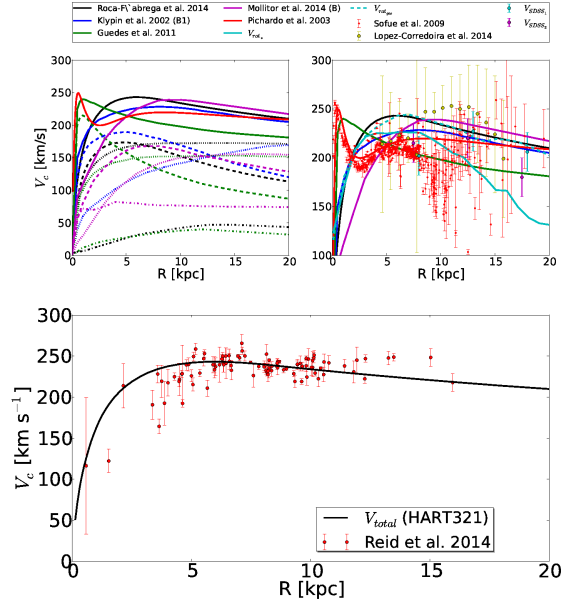


Figure 1: Top-left: Circular velocity curve of our simulated Milky Way sized galaxy model HART321 (black), ERIS simulation [9] (green), Klypin B1 model [13] (blue), Mollitor model [17] (magenta) and Pichardo analytical model [18] (red). The figure shows the contribution to the circular velocity $V_c = \sqrt{GM_{<r}/r}$ of the various mass components: dark matter (long dashed curve), stars (dotted), gas (short-dashed) and total mass (solid curve). Top-right: Total velocity curves of the same models shown at left, observational data points and gas and stars rotation curves of our model HART321. Data points come from two realizations of the rotation curve of the Milky Way from observations of blue horizontal-branch halo stars in the SDSS [22], in cyan and magenta dots, from Lopez-Corredoira [16], in green, and from Sofue [21], in red. The cyan lines show velocity rotation curves of stars and gas in our model. Bottom: Observational circular velocity curve obtained using massive young star forming regions of the MW [20]. The total V_c of our model HART321 at $z = 0$ is shown as a black solid line.

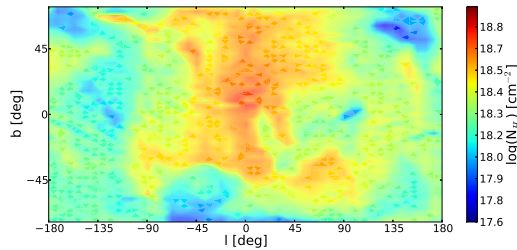


Figure 2: Hot gas ($T > 3 \times 10^5$ K) column density (top) in a full sky view of simulation HART321 in galactic coordinates, at $z = 0$.

N_{obs}	6	12	24	48	96	192	384	768	1536
σ_{N_H} [10^{18} cm $^{-2}$]	0.355	0.252	0.179	0.125	0.087	0.064	0.044	0.031	0.023
σ_{N_H}/N_H [%]	15.6	11.1	7.9	5.5	3.8	2.8	1.9	1.4	1.0
$\sigma_{M_{\text{hotgas}}}$ [10^{10} M $_{\odot}$]	0.195	0.136	0.096	0.067	0.046	0.034	0.024	0.016	0.012
$\sigma_{M_{\text{hotgas}}}/M_{\text{hotgas}}$ [%]	16.3	11.3	8.0	5.6	3.8	2.8	2.0	1.3	1.0

Table 1: Standard deviations and relative error of the hot gas column density distribution and of the total mass obtained using N observations randomly distributed in the sky.

mass with a relative error, computed as σ/M_{hotgas} , lower than 5%.

To undertake such studies we have located our mock observer at 8 kpc from the galactic center, inside the galactic plane and at a random azimuthal angle. Next we have made a hot gas column density histogram using 2500 lines of sight (20 deg 2 each), covering the full sky. We observe the hot gas column density follows a distribution function peaked at $\log(N_H) = 18.204$ with a higher dispersion in the high density region. We have made 10^5 independent experiments in where we have computed the mean of the column density distribution that results from observing 6, 12, 24, 48, 96, 192, 384, 768 and 1536 Monte Carlo randomly distributed directions, each time. For each set of 10^5 experiments we have computed the mean of the $\langle N_H \rangle$ and its standard deviation. It can be demonstrated that standard deviations presented here include both, the intrinsic error due to inhomogeneities of the distribution and the error introduced because of using a low number of observations. Preliminary results from this experiment are presented in Table 1 where we can see that between 50 and 100 random directions are needed to recover the total hot gas mass with a relative error lower than 5%.

Although a more refined statistical analysis is in progress, from this work we conclude that the number of observations that are commonly used in the bibliography is not high enough to ensure a good computation of the total baryonic mass in galaxies. In the future we will add to our studies the effect of observational constraints such as avoiding the disk plane. We will also add the effects of using other assumptions that are usual in observational works and that have not been studied here.

3.2 Two misaligned bars

When analysing the structure parameters of models HART321, HART322 and HART323 (see Table 6.1 in Roca-Fàbrega PhD thesis) we have detected the presence of two misaligned stellar bars in the disk region. We have analysed their evolution from $z = 3$ to $z = 0$ and we have found that one bar is young and has been formed from secular evolution of disk particles in the last 8 Gyr while the other one is old and has a completely different origin. The origin of the old bar is a major merger at $z = 3$, thus it is a fossil of this event.

These two bars are misaligned near 90 deg and the younger is much shorter and concentrated than the older that is longer and less dense in the central region. The rotation frequencies of both bars are similar. These two results, although preliminary, suggest that the configuration

we observe in our simulation could be stable for a long time as the interaction between both components is small. Recently it has been made a theoretical exercise [7] in where it was concluded that a system with two similar bars misaligned by 90 deg can be stable. It will be very interesting to investigate deeply if such configuration exists in nature and under which conditions.

References

- [1] Agertz, O., Teyssier, R., Moore, B. 2011, MNRAS, 410, 1391
- [2] Aumer, M., White, S. D. M., Naab, T., Scannapieco, C. 2013, MNRAS, 434, 3142
- [3] Boylan-Kolchin, M., Bullock, J. S., Sohn, S. T., Besla, G., van der Marel, R. P. 2013, ApJ, 768, 140
- [4] Brooks, A. M., Solomon, A. R., Governato, F., McCleary, J., MacArthur, L. A., Brook, C. B. A., Jonsson, P., Quinn, T. R., Wadsley, J. 2011, ApJ, 728, 51
- [5] Dutton, A. A., Conroy, C., van den Bosch, F. C., Prada, F., More, S. 2010, MNRAS, 407, 2
- [6] Feldmann, R., Carollo, C. M., Mayer, L. 2011, ApJ, 736, 88
- [7] Garzon, F. & Lopez-Corredoira, M. 2014, ArXiv e-prints
- [8] Governato, F., Brook, C., Mayer, L., et al. 2010, Nature, 463, 203
- [9] Guedes, J., Callegari, S., Madau, P., Mayer, L. 2011, ApJ, 742, 76
- [10] Gupta, A., Mathur, S., Krongold, Y., Nicastrò, F., Galeazzi, M. 2012, ApJl, 756, L8
- [11] Gupta A., Mathur S., Galeazzi M., Krongold Y., 2014, APSS
- [12] Kafle, P. R., Sharma, S., Lewis, G. F., Bland-Hawthorn, J. 2014, ApJ, 794, 59
- [13] Klypin, A., Zhao, H., Somerville, R. S. 2002a, ApJ, 573, 597
- [14] Kravtsov, A. V., Klypin, A. A., Khokhlov, A. M. 1997, ApJS, 111, 73
- [15] Kravtsov, A. V. 2003, ApJ, 590, L1
- [16] López-Corredoira M. 2014, A&A, 563, A128
- [17] Mollitor, P., Nezri, E., Teyssier, R. 2014, ArXiv e-prints
- [18] Pichardo, B., Martos, M., Moreno, E., Espresate, J. 2003, ApJ, 582, 230
- [19] Piontek, F. & Steinmetz, M. 2011, MNRAS, 410, 2625
- [20] Reid, M. J., Menten, K. M., Brunthaler, A., et al. 2014, ApJ, 783, 130
- [21] Sofue, Y., Honma, M., Omodaka, T. 2009, PASJ, 61, 227
- [22] Xue, X. X., Rix, H. W., Zhao, G., et al. 2008, ApJ, 684, 1143
- [23] Zemp, M. 2013, ArXiv e-prints